PLASMA WAKEFIELD START TO END ACCELERATION SIMULATIONS FROM PHOTOCATHODE TO FEL WITH SIMULATED DENSITY PROFILES*

A. Marocchino[†], E. Brentegani, A. Biagioni, E. Chiadroni, M. Ferrario,
A. Giribono, F. Filippi, R. Pompili, C. Vaccarezza, INFN-LNF, Frascati, Italy
A. Cianchi, University of Rome Tor Vergata, Rome, Italy
A. Bacci, A. R. Rossi INFN Milano, Milano, Italy
V. Petrillo, Università di Milano, Milano, Italy

Abstract

Plasma Wakefield acceleration is a promising new acceleration technique that profits by a charged bunch, e.g. an electron bunch, to break the neutrality of a plasma channel to produce a wake where a trailing bunch (or witness) is eventually accelerated. The quest to achieve extreme gradient conserving high brightness has prompted to a variety of new approaches and techniques. Most of the proposed schemes are however limited to the only plasma channel, assuming in the vast majority of cases, ideal scenarios (e.g. ideal bi-gaussian bunches and uniform density plasma channels). Realistic start-to-end simulations, from the photo-cathode to FEL via a high gradient, emittance and energy spread preserving plasma section, are mandatory for paving the way towards plasma-based user facilities.

INTRODUCTION

Plasma-based accelerators (PBAs) represent, today, a new frontier for the development of compact advanced radiation sources and next generation linear colliders. High brightness electron beams are the future goal of such kind of accelerators, a new technology that is envisioned to compete with the RF technology. Since the very first conception [1] great effort (with equivalent progress) has been placed [2–8] to demonstrate the acceleration of electron beams with gradients of the order of several tens of GV/m, produced either by a laser drive (LWFA) or with a particle driven (PWFA). In PWFA the high gradient wakefield is induced by a high-energy charged particle beam (referred to as driver bunch) travelling through a pre-ionised plasma. The background electrons by shielding the charge breakup produced by the driver induce an accelerating field. The second bunch (referred to as trailing bunch or witness) placed on the right phase is so accelerated by the induced electric field [9–11].

The aforementioned publications indicate that either LWFA and PWFA are capable to produce strong accelerating gradients, but do not address the issue of beam acceleration with quality retention. In other words, the capability for a PWFA scheme to accelerate a trailing bunch with an acceptable quality for any scientific applications, such a Free Electron Laser (FEL) or a future particle-particle collider, or even for medical applications is still an open question.

The work presented in this proceeding tries to address the problem of quality bunch transport numerically for a PWFA scheme. The scheme proposed leverages on the well establish RF know-how to produce and manipulate the bunches to match the strict plasma matching requirements, so that, once injected into the plasma the trailing bunch is boosted to the desired energy. The scheme can thus be decoupled into two parts. A first stage aims in generating two electron bunches (the driver and the trailing bunch) with a given time-separation so that once injected into the plasma they will be at right phase to maximize acceleration. The generation, distance positioning and acceleration is achieved using the COMB [12] technique and an RF in the X-band regime, for a final particle energy of 500 MeV. The plasma with a 10^{16} cm^{-3} number density is confined by a millimeter diameter capillary and ionized with plasma discharges, accelerates the particles from 500 MeV to 1 GeV in about 30 cm. The particle extracted from the plasma accelerating section are then injecting into a FEL. The evolution of the beam, from the photo-injector to the FEL via the plasma cell, is performed with a *single* simulation by concatenating several codes used to addressed the different physics occurring in the different accelerating section. We refer to this single simulation as a *start-to-end* simulation. This work is part of EuPRAXIA [13, 14] (European Plasma Research Accelerator with eXcellence In Applications) European project whose final goal is to use PBA to seed a FEL for physical and biological applications. Specifically EuPRAXIA@SPARC_LAB [14] is the envisioned EuPRAXIA European Italian-located facility operating at 1–5 GeV for FEL experiments.

SECTION I: INJECTOR

A comb-like configuration for the electron beam is used to generate simultaneously a 200 pC driver followed by a 30 pC trailing bunch. The comb-like operation foresees the generation of two or more bunches within the same RF accelerating bucket through the so-called laser-comb technique [12, 15] consisting in a train of laser time-spaced pulses illuminating the photo-cathode. The witness arrives earlier than the driver on the photo-cathode and then they are reversed in time at the end of the velocity bunching process, during

---

MOPAG01

A-2 Modeling of Current and Future Machines

which the longitudinal phase space is rotated. Experimental results have been obtained at SPARC_LAB where the laser-comb technique is routinely used in order to produce trains of multiple electron bunches [16] for narrow-band THz generation [17], two-color FEL experiments [18, 19] and resonant particle driven PWFA [20]. Computational studies have been dedicated to provide two bunches separated by 0.55 ps [21], which corresponds to $\lambda_p/2$, where $\lambda_p = 330\,\mu$m for $n_p = 10^{16}$ cm^{-3}. Both driver and witness bunches must be compressed down to 50 fs and 10 fs (FWHM), respectively. The process need some fine tuning to avoid emittance growth, naturally occurring because of the witness-driver overlapping during the velocity bunching regime. The photocathode laser has been shaped in order to provide at the cathode a witness and a driver bunches separated by Δt=4.8 ps. With this configuration the beam crossing occurs in the second TW accelerating cavity and a fine-tuning of the RF phases suffices to provide the desired 0.55 ps beam separation corresponding to $\lambda_p/2$. Gaussian longitudinal distribution with σ_z =120 μm (RMS) and uniform transverse distribution of radius $r = 0.35$ mm have been assumed for the witness pulse at the cathode. The different intensities between the two pulses permit to generate bunches with different charges: a 30 pC trailing bunch and a 200 pC driver. It is worth to notice by adopting a σ_D=0.35 mm, the FWHM witness length does not suffer lengthening, although the minimum RMS witness length is obtained for σ_D=0.25 mm. The sliced current at the end of the photo-injector line is plotted in Fig.1.
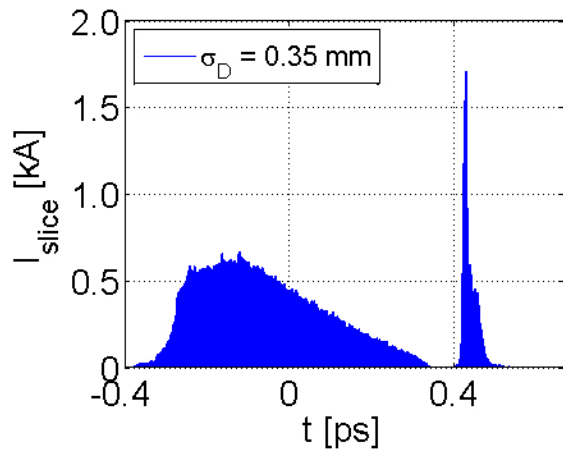

Figure 1: Driver and trailing bunch longitudinal current distribution at the photo-injector exit. The beam is propagating from right to left with the driver arriving earlier than the trailing bunch.

Driver and trailing bunch have been simulated with the TSTEP code and with 30k and 200k macro-particles respectively. In the described configuration the driver arrives 0.58 ps earlier than the witness at the X-band booster. It is worth to notice that the trailing bunch length is about 3 μm FWHM with a normalized transverse emittance of ~0.7 mm mrad.

SECTION II: LINAC

The X-band RF linac is used to accelerates the entire beam to 500 MeV [22, 23], energy of the beam entering the plasma, specifically the trailing bunch is prepared for plasma injection with a transverse dimension of 1-2 μm spot size. The comb-like electron beam undergoes deep over-compression in the photo-injector by means of the velocity bunching scheme. The same accelerating gradient of $E_{acc} \approx$ 20–36 MV/m is applied in L1 and L2 linac section respectively, and the final electron beam energy is $E_{L2exit} \approx$ 580 MeV, with an energy spread less than 0.1%. The driver and witness bunches are characterized by high charge/low current and low charge/high current, respectively. Moreover, the initial matching conditions for the injection in the X-band linac are quite different for the two bunches, as shown by their transverse phase space at the linac entrance (i.e. injector exit). In this regard, an efficient sharing of the same lattice is achieved by means of a mild transverse focusing that aims to keep the RMS size of the comb beam compatible with the beam stay-clear-aperture through all the X-band accelerator. The same argument applies also to the focusing stage with the permanent quadrupoles at the entrance of the plasma capillary where a residual asymmetry between horizontal and vertical plane for the witness beams is present, see Fig. 2.
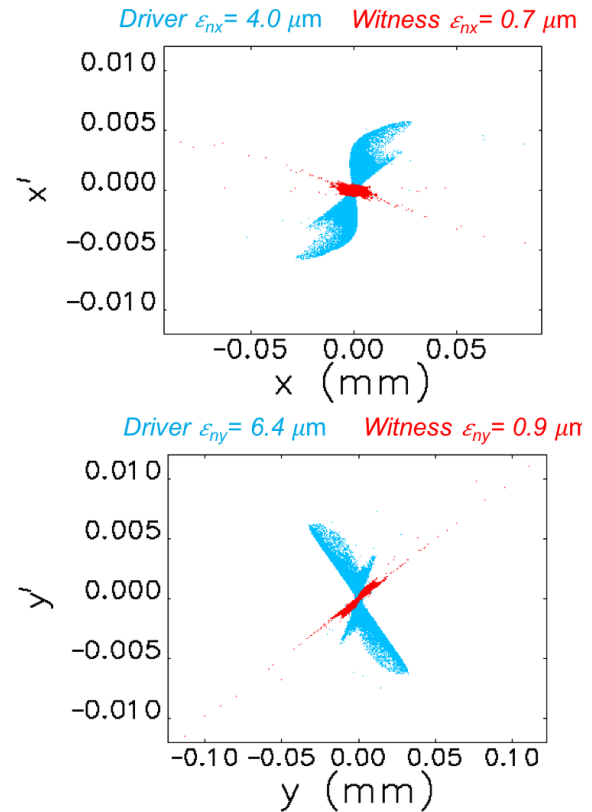

Figure 2: Horizontal and vertical phase space distribution of the PWFA driver (cyan dot) and witness (red dot) beams at the capillary entrance.

SECTION III: THE PLASMA CELL

Start-to-end simulations use, for the plasma section, the state-of-the-code ARCHITECT [24, 25]. The use of Architect has been dictated by the necessity to run long simulations where a classical particle-in-cell (PIC) approach would have been computationally too expensive. The Architect reduced model, which relies on a fluid background, has been benchmarked numerically against the ALaDyn-PWFA [26] PIC code [25] and versus SPARC_LAB experimental results [27, 28]. Start-to-end simulations are performed by concatenating the use of codes without any phase space manipulation or remapping. Specifically, for the interface RF X-band with plasma The ELEGANT code is used to track particle up to the plasma entrance, the particle phase-space is then imported into the Architect code for the evolution in the plasma section. Simulations described in this section have been run with a longitudinal resolution of 1 μm and a transverse resolution of 0.4 μm, a mesh that allows to resolve the fine structure with a reasonable computational cost. The advancing time step is of 1.1 fs. The number of particle used to discretize the driver is, on average, 30 particles per cell while the witness is discretized with an average of 100 particle per cell. We recall that the goal is to accelerate the trailing bunch retaining as much as possible its original quality. To limit the energy spread growth, the trailing bunch has been designed with a (as much as possible) *triangular* shape. The triangular shape together with a specific value of peak charge represents the optimized longitudinal density profile that limits energy growth spread during propagation. Driver and witness have been designed to perform the best acceleration in terms of quality and in terms of energy transfer (*transformer ratio, R*) [29], parameter that identifies the rate of energy transfer from the driver to the witness. In our case the transformer ratio in estimated in the range 2-3. The foreseen experiment is planned in the so-called weakly-non-linear regime, where despite fields resemble a sawtooth profile linear field sum is still possible. The parameter we used to measure the degree of nonlinearity is the *reduced charge parameter* [30, 31], $Q = \frac{N_b}{n_0} \kappa_p^3$, with N_b the electron bunch number (bunch charge divided by the elementary charge). For this case the driver reduced charge is $Q \sim 0.8 - 0.9$.

Nonetheless, if the upstream application is a FEL application that requires a slice current around 2 kA, combining this requirement with the triangular shape, simulations helps identifying that beam loading compensation occurs for a driver-witness distance 184 μm or $0.55 \times \lambda_p (n_0 = 10^{16})$, where the electric field experienced by the witness is around 1.1 GV/m. We recall that the accelerating field together with the plasma wavelength depend upon the plasma number density n_0, $\propto n_0^{1/2}$ and $\propto n_0^{-1/2}$ respectively. The capability to control the density would permit some flexibility and adjustments in the bubble profile and accelerating fields, this to compensate -on site- whenever the distance between driver and witness would oscillate or change for experimental unforeseen reasons. The flat density profile, together with the

required value is achieved with a capillary tube. The capillary tube, confining the ejected gas, permits a high degree of control to which we can rely on for experimental on site optimization. At present simulations consider some density ramps of the order of 0.5 cm, that are experimentally reasonable and whose length is below the betatron wavelength assuring no bunch oscillations within the ramps to increase acceleration robustness [26]. At plasma entrance, the trailing bunch is delivered with a shape that resemble the triangular required shape, transversally the bunch is fairly symmetric in size and in emittance Table 1.

Table 1: PWFA Bunch Parameters at Plasma Entrance and at Plasma Exit (the best slice value is also reported)

Beam	units	Driver IN	Driver OUT	Tr. B. IN	Tr. B. OUT
Charge	pC	200	200	30	30
σ_x	μm	8	6.4	1.47	1.42
σ_y	μm	3.1	10	3.17	1.4
σ_z	μm	52	50	3.85	3.8
ε_x	μm	2.56	4.1	0.6	0.96
ε_y	μm	4.8	11.4	0.55	1.2
σ_E	%	0.2	20	0.07	1.1
E	MeV	567	420	575	1030
Best Slice					
current	kA			2	2.0
ε_x	μm			0.59	0.57
ε_y	μm			0.58	0.62
σ_E	%			0.011	0.034

The driver is instead of lower brightness quality, but since the driver will undergo depletion -anyway- we can accept a lower quality since its main purpose is to *only* drive the wake. The setting of the RF line in favor of the witness naturally bring the driver on a less optimized point that is delivered at plasma with a lower quality than the trailing bunch. The driver at plasma entrance has the front part that is highly convergent, convergence that will cause a consequent expansion within the plasma channel producing a unique funnel shape, Fig. 3. The driver is capable to induce a weakly nonlinear wake with an effective maximum field that peaks (at bubble closure) around 2.5–3.0 GV/m, as can been retrieved from Fig. 3. The central part of the driver that mostly contributes to generate the wake looses after 40 cm about 150 MeV, the witness gains about 460 MeV. The slice analysis, reported numerically in Table 1 suggests that the witness head and tail undergo a phase space dilution, while the central slice with very high current retain high quality. The witness, at plasma entrance, has the emittance in both planes as well as the energy spread almost uniform along the entire witness length. After the plasma acceleration section, the bunch has lost this homogeneity exhibiting a different slice quality along its length.

The front part and the read part of the witness are characterized by large emittance and energy spread. While ideally
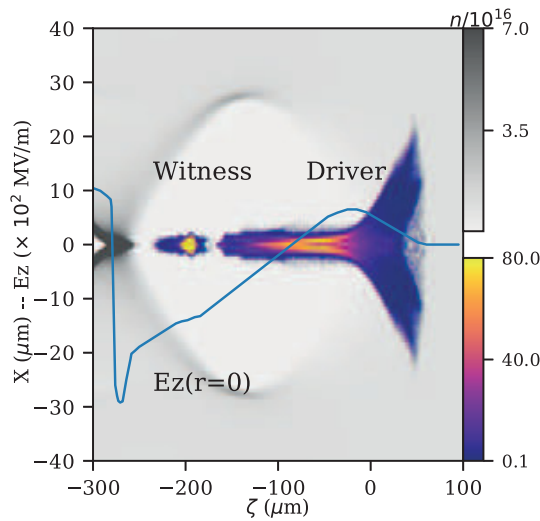
Figure 3: Bunch and background density colormaps after 5 mm within the plasma. The bunch density is plotted with a *plasma* colormap, while the background is plotted with a grey colormap. The longitudinal accelerating electric field, on axis, is over-imposed with a solid blue line. For scale purposes and for sake of clarity the Ez is plotted in hundreds of MV/m.

we wish to conserve quality all along the trailing bunch, the head and tail are characterized by a lower current, condition that allows us some flexibility on these regions since their lasering within the FEL would be negligible. However, and most importantly, the region within the high current bell retains its quality. From Fig. 4, top panel, we notice that under the region of high current the emittance in both plane is almost conserved with little deterioration. The energy spread undergoes some general increase also in the region of maximum current. The slice value, in the region of maximum current, stays below 0.1%. The peak current value corresponds to the transition from a higher value to the lowest one. The best slice characterized by a 2 kA current, has an energy spread as low as 0.034%, an emittance of 0.57 mm−mrad and 0.62 mm−mrad in the x and y plane respectively.
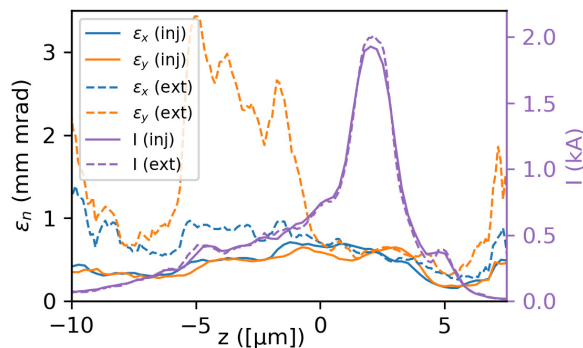

Figure 4: Slice analysis for the witness bunch at plasma input, dashed color, and at plasma exits, solid color.

The Architect Code

One of the codes used to complete the start-to-end simulations is the ARCHITECT code used to study the bunch dynamics within the plasma. ARCHITECT integrates plasma wakefield acceleration equation by combining a PIC approach with fluid equations. The PIC approach is used to discretise the electron bunches while the background electrons are treated as a cold fluid, electromagnetic fields are evolved accordingly to Maxwell's equations. The set of equations solved can be written, in a compact way, as follows,

$$
\begin{aligned}
\partial_t n_e + \nabla \cdot (\boldsymbol{\beta}_e c\, n_e) &= 0 \\
\partial_t \mathbf{p}_e + c\boldsymbol{\beta}_e \cdot \nabla \mathbf{p}_e &= q(\mathbf{E} + c\boldsymbol{\beta}_e \times \mathbf{B}) \\
\nabla \times \mathbf{E} + \partial_t \mathbf{B} &= 0 \\
\nabla \times \mathbf{B} - c^{-2}\partial_t \mathbf{E} &= q\mu_0 c\,(n_e \boldsymbol{\beta}_e + n_b \boldsymbol{\beta}_b) \\
d_t \mathbf{p}_{\text{particle}} &= q(\mathbf{E} + c\boldsymbol{\beta}_{\text{particle}} \times \mathbf{B}) \\
d_t \mathbf{x}_{\text{particle}} &= \mathbf{v}_{\text{particle}}
\end{aligned}
\tag{1}
$$

where $\mathbf{E}$ is the electric field, $\mathbf{B}$ the magnetic field, c the speed of light, $\boldsymbol{\beta}_e = \mathbf{u}_e/c$ the relativistic β for the background electrons, $\boldsymbol{\beta}_b$ the relativistic β for the electron bunch, $\mathbf{p}_e$ the fluid relativistic momentum for electrons, n_e is the electron density and n_b the bunch density. For each single particle of the kinetic bunch(es) we identify a relativistic momentum, $\mathbf{p}_{\text{particle}}$, a relativistic beta, $\boldsymbol{\beta}_{\text{particle}}$, a velocity, $\mathbf{v}_{\text{particle}}$, and a position, $\mathbf{x}_{\text{particle}}$. The first and second equations of Eq. (1) are the fluid mass conservation and the fluid momentum conservation respectively. The third and the fourth are Faraday's law and Ampere's law respectively. The last two equations of Eq. (1) are the kinetic compound to the model, the relativistic Newton's law for each single particle composing the bunch(es): the momentum equation and the position-velocity equation. In Eq. (1) the fluid velocity classically written as $\mathbf{u}_e$ has been written as a function of β. Ions are assumed as a static background.

Dynamic in plasma-based accelerators spans over a large range of timescales, while beams evolve on a timescale on the order of the inverse betatron oscillations, the background plasma evolves on a timescale on the order of the inverse of the plasma frequency. The shortest dominating timescale is the background plasma frequency, by using a fluid description we drastically reduce the computational costs in a variaty of mean: from memory occupations to evolution costs since fluid algorithms are less expensive than a 3D3V particle evolution.

The hybrid approach algorithmic strength consists on the combination of mature state-of-the-art numerical techniques both for the kinetic description as well as for the fluid part. The hybrid approach leverage on the wise combination of the different algorithms using different timescales. The interaction between the kinetic and fluid scale is made possible via the bunch current, calculated and weighted on the fluid mesh. The novelty introduced by architect is the resolution of evolution equation in a time explicit domain, there is no quasi-static approximation. Moreover electron bunches are

MOPAG01

initialized in vacuum with their self consistent field, we treat the transition from vacuum to plasma.

SECTION IV: FEL

The electron beam accelerated by plasma are then transported to an ondulator and photon production is studied with the use of the GENESIS [32] code. Considering a $a_w = 0.8$, the resonant wavelength is $\lambda = 2.987$ nm. The matching to the undulator leads to σ_x=40.6 µm and σ_y=28.6 µm with the quadrupoles 9 cm long and set at 18 T/m. The FEL parameter results to be $\rho = 2.51 \times 10^{-3}$, its 3D value is $\rho_{3D} = 1.86 \times 10^{-3}$ for $L_{g,3D}$=0.37 m. Simulations predicts The growth of the radiation, as given by simulations with GENESIS 1.3 [32], is shown in Fig. 5. The saturation length is about 15-25 m with emitted energy 6.5 µJ at 30 m, for a photon flux of 9.76×10^{10} per shot. The minimum bandwidth value, achieved at 20 m is 0.3%, while at 30 m saturation effects have increased it at 0.9%. Finally, the nominal case a1 has been worsened in current, emittance and energy spread by 5% and 10%, we observe a decrease in the emission respectively of 8% and 13%.
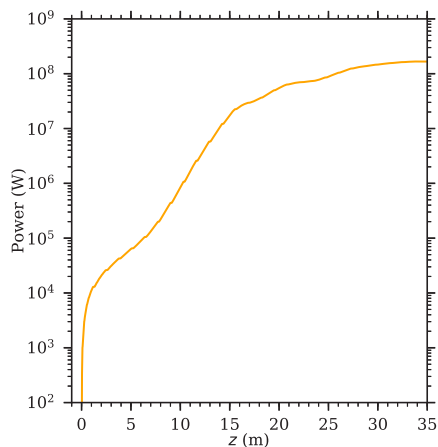

Figure 5: FEL radiation growth along the undulator length.

CONCLUSION

This work focuses on a start-to-end simulations for a FEL machine, driven by a PWFA accelerator whose bunch is generated and accelerated by a RF photo-injector. The RF photo-injector and the subsequent X-band boosting line had been tuned to deliver to the plasma a driver able to accelerated a trailing bunch from 0.5 GeV to 1 GeV by preserving the quality of its core so to well laser inside a FEL machine. The simulation is possible by combining in cascade a series of codes, each devoted to reproduce the relevant physics in the given section.

ACKNOWLEDGEMENTS

REFERENCES

[1] T. Tajima and J. M. Dawson, "Laser electron accelerator," *Physical Review Letters*, vol. 43, no. 4, pp. 267–270, 1979.

[2] S. Corde *et al.*, "Multi-gigaelectronvolt acceleration of positrons in a self-loaded plasma wakefield," *Nature*, 2015.

[3] M. Litos *et al.*, "High-efficiency acceleration of an electron beam in a plasma wakefield accelerator," *Nature*, vol. 515, no. 7525, pp. 92–95, 2014.

[4] W. P. Leemans *et al.*, "Gev electron beams from a centimetre-scale accelerator," *Nature Physics*, vol. 2, no. 10, pp. 696–699, 2006.

[5] H. Schwoerer *et al.*, "Laser-plasma acceleration of quasi-monoenergetic protons from microstructured targets," *Nature*, vol. 439, no. 7075, pp. 445–448, Jan. 2006.

[6] I. Blumenfeld *et al.*, "Energy doubling of 42 GeV electrons in a metre-scale plasma wakefield accelerator," *Nature*, vol. 445, no. 7129, pp. 741–744, Feb. 2007.

[7] P. Muggli *et al.*, "Generation of Trains of Electron Microbunches with Adjustable Subpicosecond Spacing," *Physical Review Letters*, vol. 101, no. 5, p. 054801, Aug. 2008.

[8] E. Kallos *et al.*, "High-Gradient Plasma-Wakefield Acceleration with Two Subpicosecond Electron Bunches," *Physical Review Letters*, vol. 100, no. 7, p. 074802, Feb. 2008.

[9] S. Van der Meer, "Improving the power efficiency of the plasma wakefield accelerator," *CERN-PS-85-65-AA. CLIC-Note-3*, 1985.

[10] T. Katsouleas, "Physical mechanisms in the plasma wake-field accelerator," *Physical Review A - General Physics*, vol. 33, no. 3, pp. 2056–2064, Mar. 1986.

[11] J. B. Rosenzweig *et al.*, "Acceleration and focusing of electrons in two-dimensional nonlinear plasma wake fields," *Physical Review A (Atomic*, vol. 44, no. 1, pp. R6189–R6192, Nov. 1991.

[12] M. Ferrario, D. Alesini, A. Bacci, M. Bellaveglia, R. Boni, M. Boscolo, P. Calvani, M. Castellano, E. Chiadroni, A. Cianchi *et al.*, "Laser comb with velocity bunching: Preliminary results at sparc," *Nuclear Instruments and Methods in Physics Research Section A: Accelerators, Spectrometers, Detectors and Associated Equipment*, vol. 637, no. 1, pp. S43–S46, 2011.

[13] P. A. Walker *et al.*, "Horizon 2020 EuPRAXIA design study," *Journal of Physics: Conference Series*, vol. 874, p. 012029, Jul. 2017.

[14] M. Ferrario *et al.*, "Eupraxia@sparc_lab design study towards a compact fel facility at lnf," *Nucl. Instrum. Meth.*, 2018. http://www.sciencedirect.com/science/article/pii/S0168900218301414

[15] F. Villa *et al.*, "Laser pulse shaping for high gradient accelerators," *Nuclear Instruments and Methods in Physics Research Section A: Accelerators, Spectrometers, Detectors and Associated Equipment*, vol. 829, pp. 446–451, 2016.

[16] A. Mostacci *et al.*, "Advanced beam manipulation techniques at sparc," in *IPAC 2011-2nd International Particle Accelerator Conference*, 2011, pp. 2877–2881.

[17] F. Giorgianni *et al.*, "Tailoring of highly intense thz radiation through high brightness electron beams longitudinal manipulation," *Applied Sciences*, vol. 6, no. 2, p. 56, 2016.

[18] V. Petrillo, M. Anania, M. Artioli, A. Bacci, M. Bellaveglia, E. Chiadroni, A. Cianchi, F. Ciocci, G. Dattoli, D. Di Giovenale *et al.*, "Observation of time-domain modulation of free-electron-laser pulses by multipeaked electron-energy spectrum," *Physical Review Letters*, vol. 111, no. 11, p. 114802, 2013.

[19] A. Petralia *et al.*, "Two-color radiation generated in a seeded free-electron laser with two electron beams," *Physical review letters*, vol. 115, no. 1, p. 014801, 2015.

[20] E. Chiadroni and at al., "Beam manipulation for resonant plasma wakefield acceleration," *Accept. Nucl. Instrum. Meth.*, vol. 865, pp. 139–143, 2017.

[21] A. Giribono *et al.*, "Eupraxia@sparc_lab: the high-brightness rf photo-injector layout proposal," *Accept. Nucl. Instrum. Meth.*, 2018.

[22] C. Vaccarezza *et al.*, "Eupraxia@sparc_lab: Beam dynamics studies for the x-band linac," *Accept. Nucl. Instrum. Meth.*, 2018.

[23] M. Diomede *et al.*, "Rf design of the x-band linac for the eupraxia@sparc_lab project," in *Proceedings IPAC 2018*, 2018.

[24] A. Marocchino *et al.*, "Efficient modeling of plasma wakefield acceleration in quasi-non-linear-regimes with the hybrid code Architect," *Nuclear Instruments and Methods in Physics Research Section A: Accelerators, Spectrometers, Detectors and Associated Equipment*, vol. 829, pp. 386–391, sep 2016.

[25] F. Massimo, S. Atzeni, and A. Marocchino, "Comparisons of time explicit hybrid kinetic-fluid code Architect for Plasma Wakefield Acceleration with a full PIC code," *Journal Of Computational Physics*, vol. 327, pp. 841–850, 2016.

[26] A. Marocchino *et al.*, "Design of high brightness Plasma Wakefield Acceleration experiment at SPARC_LAB test facility with particle-in-cell simulations," *Nucl. Instrum. Meth. A*, 2018.

[27] A. Marocchino *et al.*, "Experimental characterization of the effects induced by passive plasma lens on high brightness electron bunches," *Applied Physics Letters*, vol. 111, no. 18, p. 184101, 2017.

[28] R. Pompili, M. Anania, M. Bellaveglia, A. Biagioni, S. Bini, F. Bisesto, E. Brentegani, G. Castorina, E. Chiadroni, A. Cianchi *et al.*, "Experimental characterization of active plasma lensing for electron beams," *Applied Physics Letters*, vol. 110, no. 10, p. 104101, 2017.

[29] F. Massimo, A. Marocchino, E. Chiadroni, M. Ferrario, A. Mostacci, P. Musumeci, and L. Palumbo, "Transformer ratio studies for single bunch plasma wakefield acceleration," *Nuclear Inst. and Methods in Physics Research, A*, vol. 740, no. C, pp. 242–245, mar 2014.

[30] J. Rosenzweig *et al.*, "Energy loss of a high charge bunched electron beam in plasma: Simulations, scaling, and accelerating wakefields," *Physical Review Special Topics-Accelerators and Beams*, vol. 7, no. 6, p. 061302, 2004.

[31] P. Londrillo *et al.*, "Numerical investigation of beam-driven PWFA in quasi-nonlinear regime," *Nuclear Inst. and Methods in Physics Research, A*, vol. 740, pp. 236–241, 2014.

[32] S. Reiche, "Genesis 1.3: a fully 3d time-dependent fel simulation code," *Nuclear Instruments and Methods in Physics Research Section A: Accelerators, Spectrometers, Detectors and Associated Equipment*, vol. 429, no. 1-3, pp. 243–248, 1999.